Proceedings of ITC18,2008

Status and High Power Performance of the 10-MW 140-GHz ECH System for the Stellarator W7-X

M. Thumm[1,2], P. Brand[4], H. Braune[3], V. Erckmann[3], G. Gantenbein[1], S. Illy[1], W. Kasparek[4], S. Kern[1], H. P. Laqua[3], C. Lechte[4], N.B. Marushchenko[3], G. Michel[3], B. Piosczyk[1], M. Schmid[1], Y. Turkin[3], M. Weissgerber[3] and the W7-X ECH-Teams at FZK Karlsruhe[1], IPP Greifswald[3] and IPF Stuttgart[4]

[1]*Forschungszentrum Karlsruhe, Association EURATOM-FZK,Institut für Hochleistungsimpuls- und Mikrowellentechnik, D-76021 Karlsruhe, Germany*

[2]*Universität Karlsruhe, Institut für Höchstfrequenztechnik und Elektronik, D-76131 Karlsruhe, Germany*

[3]*Max-Planck-Institut für Plasmaphysik, EURATOM Association, Teilinstitut Greifswald, D-17491 Greifswald, Germany*

[4]*Universität Stuttgart, Institut für Plasmaforschung, D-70569 Stuttgart, Germany*

During the last years, electron cyclotron heating (ECH) was proven to be one of the most attractive heating schemes for stellarators because it provides net-current-free plasma startup and heating. Both the stellarator Wendelstein 7-X (W7-X) and the ITER tokamak will be equipped with a strong ECH and current-drive system. Both ECH&CD systems are comparable in frequency and have continuous-wave (CW) capability (140 GHz, 10 MW for W7-X and 170 GHz, 27 MW for ITER). The heating- and current drive scenarios, which support W7-X operation at various magnetic fields and in different density regimes are reviewed. The ECH plant consists of ten RF-modules with 1 MW power each. The commissioning of the entire ECH installation is in an advanced state. All supporting systems like the superconducting magnets, the water cooling plant, the cryogenic plant, the main power supply and all high-voltage modulators are completed and operating. The ten gyrotrons at W7-X will be arranged in two 5 MW subgroups symmetrically to a central beam duct in the ECH hall. The mm-wave beams of each subgroup will be combined and transmitted by a purely optical multibeam-waveguide transmission line from the gyrotrons to the torus. The mm-wave power will be launched to the plasma through ten synthetic diamond barrier windows and in-vessel quasi-optical plug-in launchers, allowing each 1-MW mm-wave beam to be steered independently. The polarization, as well as the poloidal and toroidal launch angles, will be adjusted individually to provide optimum conditions for different heating and current-drive scenarios. Integrated high power CW tests of the full transmission system (except the in vessel components) were performed recently and are in excellent agreement with theory and low power measurements. The work presently concentrates on the acceptance tests of the gyrotrons, on the front end of the transmission system near the W7-X torus and on the in-vessel components.

Keywords: Nuclear Fusion, Stellarator, Steady State Operation, Electron Cyclotron Heating, Gyrotron, Quasi-Optical Transmission

1. Inroduction

Wendelstein 7-X (W7-X) is the next step in the stellarator line towards thermonuclear magnetic fusion power plants. Stellarators have inherent steady state operation capability, because the confining magnetic field is totally generated by external coils. W7-X will be equipped with a superconducting coil system and a continuously operating (CW) 140 GHz Electron Cyclotron Heating and Current Drive (ECH&CD) system with 10 MW gyrotron power. An actively pumped divertor with 10 MW heat removal capability for stationary energy and particle control will be installed after an initial testing phase using an inertially cooled divertor in pulsed operation. An ECH power of 10 MW is required to achieve reactor relevant plasma parameters [1] at the nominal magnetic field of 2.5 T. The ECH&CD operation scenarios and the status of the in-vessel components are reported in Sec. 2. Tests experiments on

author's e-mail:manfred.thumm@ihm.fzk.de, *This paper was carried out within the framework of EFDA.*

gyrotrons are summarized in Sec. 3. The ECH plant is in a well-advanced state, integrated high power tests of the transmission line are reported in Sec. 4.

2. Operation scenarios and in-vessel components

The ECH&CD system at W7-X has to fulfill many different functions. It has to provide plasma start-up, heating and current control routinely at the different resonant confining magnetic fields. It is the only heating system, which will be fully available for long-pulse operation from beginning of the experiment. For plasma start-up and "low" plasma density ($<1.2\cdot10^{20}$ m^{-3}) operation heating with the second harmonic X-mode (X2) at 140 GHz is foreseen. Its single-pass absorption is sufficiently high that nearly total absorption is guaranteed up to the cut-off density ($<1.2\cdot10^{20}$ m^{-3}). At low density plasma temperatures of above 10 keV are expected. The heating power of 10 MW should be sufficient to sustain a plasma at $1.0\cdot10^{20}$ m^{-3} with a temperature of 4 keV. X2 operation at 103.8 GHz is also envisaged (see next chapter). In addition start-up at the third harmonic (X3) will be explored. Although in stellarators neither a permanent ECCD for the plasma confinement nor any NTM- stabilization is needed, the control of the divertor strike point position requires a permanent control of the edge rotational transform iota. In addition it should be avoided that the iota profile does approach any main rational resonance. Therefore ECCD will be used for residual bootstrap current [2] compensation and iota control on a fast time scale. For long time scales (<100s) iota will be controlled by the currents in the coil system. With the installed ECH power of 10 MW up to 300 kA current can be driven at $1.0\cdot10^{19}$ m^{-3} by ECCD. Even at $1.0\cdot10^{20}$ m^{-3} an ECCD current of up to 30 kA is expected, which will be sufficient to compensate the estimated bootstrap current of about 20 kA.

The main challenge of the first experimental campaign will be to develop an operation scenario, where the slowly growing bootstrap current is continuously compensated by a well matched central and off-axis ECCD. Efficient divertor operation probably may require a plasma density well above the X2-cutoff density. Here second harmonic O-mode heating (O2) with a plasma density of up to $2.4\cdot10^{20}$ m^{-3} is foreseen [3,4]. In contrast to X2 heating O2 single-pass absorption is well below 100%. Depending on plasma density and central plasma temperature a single-pass absorption of 50-90% is expected. The similar situation is found for X3-heating (B_{res}= 1.66 T, $n_e < 1.6\cdot10^{20}$ m^{-3}), which is a promising scenario for operation at reduced confining magnetic field. An example for X3 single-pass absorption calculations with 10 MW input power is shown in Fig. 1 (top). The related electron and ion temperatures resulting from a transport code [5] are also shown.

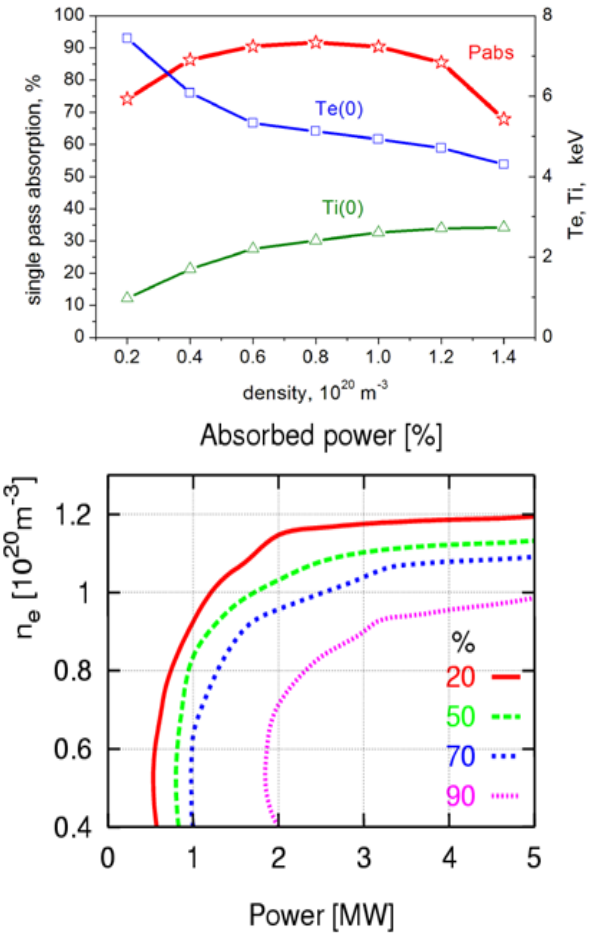

Fig. 1 Top: X3 single-pass absorption P_{abs} at 140 GHz from ray-tracing calculations as a function of the plasma density. The central electron and ion temperatures $T_e(0)$, $T_i(0)$ are also shown. Bottom: O2 triple-pass absorption at 104 GHz. Contours of constant absorbed power (in %) as a function of plasma density n_e and ECH power.

The non-absorbed part of the mm-wave beams would thermally overload the graphite tiles at the heat shield, which is opposite to the ECH antennas. Therefore several selected tiles will be replaced by specially shaped tiles made of TZM, which is a molybdenum alloy with small amounts of titanium and zirconium. These tiles reflect the mm-wave beams into a second pass through the plasma center onto a water-cooled stainless-steel reflector panel in between the ECH ports. This reflector will provide a third pass through the plasma as shown in Fig 1. (bottom)

and in Fig 2. Thus the total absorption will be significantly increased. The same reflector system can be used for the X3-heating scenario, where also an incomplete single-pass absorption is expected. The launching angle for both heating scenarios is about 12° at the position of the most elongated plasma cross-section. Therefore the beam deflection by plasma refraction is below 3 cm at the tiles, which can be easily compensated by the movable antennas. The ECCD capability at O2 will not be sufficient to compensate the bootstrap current for all magnetic configurations, but stellarator operation with a finite bootstrap current is also feasible.

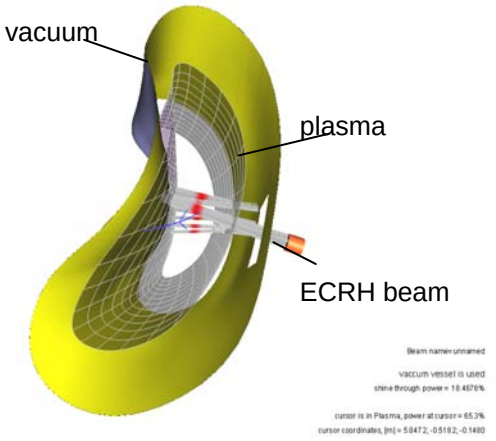

Fig. 2 Three-pass ray-tracing calculations for one selected mm-wave beam with O2-mode polarization.

For operation at ultra high plasma densities above the O-cutoff density Bernstein wave heating employing the OXB-mode conversion scenario is envisaged [6]. The transmission line and the in-vessel antennas are well designed to provide the required optimal launching angle of 55° in respect to the magnetic field direction and the nearly circular polarization. Two additional ports (N-type) are foreseen at W7-X for special ECH physics experiments with two mm-wave beams (2 MW). Here the beams will propagate along the B=const surfaces in order to localize the interaction in the phase space. Therefore advanced ECCD scenarios with supra-thermal electrons can be investigated. In addition, the N-port is also foreseen as the mm-wave injection port for the Collective Thomson Scattering diagnostics (CTS).

The in-vessel components will enable the above mentioned operational scenarios. The design of the front steering ECH antennas is compatible with full power CW requirements. Four antenna plugs are under construction, each block can handle three mm-wave beams (incl. two spare beam lines for a possible later upgrade) as shown in Fig. 3. The movable mirrors allow a poloidal steering range of ±25° and a toroidal steering range between ±15° and ∓35°, which complies with all operation scenarios.

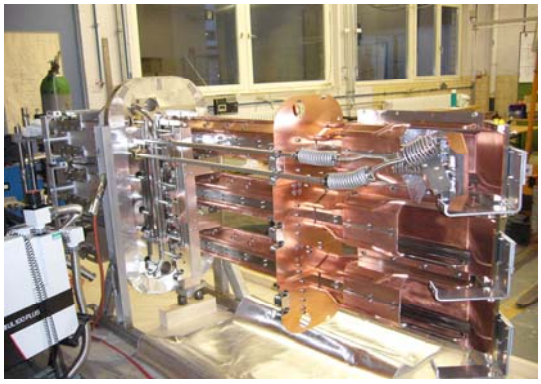

Fig. 3 Photo of the assembly of one of the four ECH antenna plugs.

The critical antenna components like the ceramic bearings and the flexible tube spirals for the cooling water supply had been already successfully tested in a mechanical mock-up under vacuum conditions and in ECH stray radiation environment. The mirror design is identical with the well proven transmission-line type. Most of the antenna components are already manufactured and the assembly has started (see Fig. 3).

The N-ports are very narrow and a remote steering scheme [7] will therefore be employed which is based on the imaging properties of a square corrugated waveguide. A solution with a bent waveguide was chosen. This makes the integration of the waveguides easier and provides a lower antenna beam divergence due to an increased waveguide cross-section. However, thorough optimization of the position of the miter bend and the vacuum valve in the waveguide are required.

The TZM reflectors for O2 and X3 heating scenarios have to sustain a mm-wave power of 0.5 MW on a surface of 120 cm^2 each. High power test (0.5 MW) of a prototype tile mounted on the original W7-X cooling plate showed an absorption of 0.3% which is in agreement with the theoretical value calculated from the material properties. With the resulting thermal load of 1.5 kW the tile reached after 200 s a steady state temperature of 470 °C at the surface and 390 °C at the cooling plate, which is acceptable for W7-X operation.

Reliable ECH operation requires special ECH-related diagnostics. The beam direction, its polarization and the absorbed power should be known with a high precision. In particular the latter is one of the most important plasma parameters, since the energy confinement time is the ratio of plasma energy and absorbed heating power.

120 pick-up antennas (open circular waveguides), which are incorporated in the heat shield tiles, will serve as diagnostics. These mono-mode waveguide tubes are combined into four bundles, which run along the vacuum vessel wall towards four B-type ports, where the signal is transmitted through the vacuum-air interface. Any contribution to the original polarization due to multiple waveguide bending will be compensated by appropriate phase shifters before the signal is detected by mm-wave diodes. A prototype of a waveguide bundle was already manufactured and is ready for a test assembly inside the W7-X vacuum vessel (see Fig. 4). The total absorbed power will be measured by at least five sniffer probes located in each of the five stellarator modules. These detectors measure the none-absorbed ECH stray radiation, which is distributed inside the vacuum vessel. Its signal will be used to detect any unintended reduction of ECH absorption in order to avoid severe machine damage of inappropriately armored in-vessel components by direct beam irradiation or mm-wave stray radiations. In addition it is planned to monitor the heat shield, which is opposite to the ECH antennas, by infrared cameras.

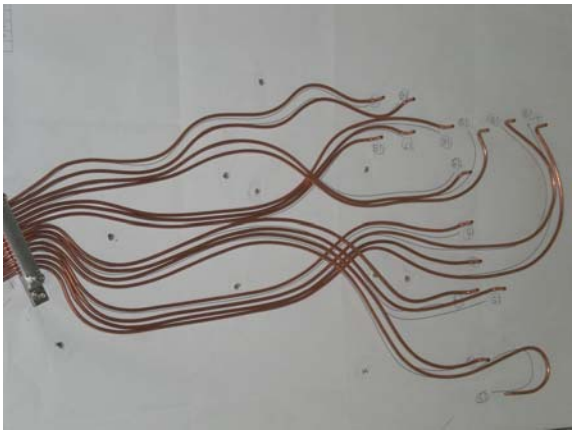

Fig. 4 Pre-shaped waveguide bundle prototype for assembly and routing tests inside the W7-X vacuum vessel.

3. Gyrotron testing and two-frequency operation

The first series gyrotron SN1 manufactured by Thales Electron Devices (TED) has been tested successfully at FZK and IPP in 2005. It has fulfilled all the specifications (0.91 MW in fundamental Gaussian mode, 30 min. pulse duration, 45% efficiency). During the acceptance test no specific limitations were observed. In order to keep the warranty this gyrotron has been sealed, the two equally performing prototype gyrotrons are routinely used for test experiments on advanced ECH components.

The next series gyrotrons showed a more or less different behavior with respect to parasitic oscillations excited in the beam tunnel region. These oscillations result in an excessive heating of the absorbing ceramic rings. The gyrotrons, re-opened after operation, showed significant damages due to overheating at the ceramic rings and the brazing of the rings. This limited in general the pulse length in full power operation to a few ms or the power in long-pulse operation to 0.6–0.7 MW.

In a first attempt to improve the situation, the manufacturer opened the series gyrotrons SN2 and SN3 and installed ceramic rings with a better brazing (SN2a, SN3a) and changed the sequence of the ceramic rings with different inner diameter (SN5). But both measures did not improve the situation significantly.

Therefore, FZK started in 2008 first designs to overcome this issue and to come to a more robust beam tunnel which suppresses the excitation of parasitic oscillations more efficiently. In order to validate a new beam tunnel as much as possible, it is planned to perform tests with a 170 GHz coaxial cavity gyrotron and a frequency step tunable 140 GHz gyrotron with a structurally modified beam tunnel which represents only a small change in the existing design.

In the following we will report on the experimental results obtained with the series gyrotrons SN2a, SN3a and SN5, all equipped with the original beam tunnel.

In 2008 acceptance tests have been continued with the repaired serial gyrotron SN2a at IPP Greifswald. The tube achieved 0.83 MW at 3 min and 0.71 MW at 25 min. pulse length. However, during conditioning of the tube the pressure level increased and complicated further progress. The control of the vacuum system of the gyrotron did not show a leakage. The acceptance tests of the tube were stopped by a crack of the output window which occured during operation without any alarm message from the interlock system. The gyrotron was sent back to the manufacturer for opening and detailed failure analysis.

The serial gyrotron SN3a has been tested at FZK in short pulse (~ ms) and long pulse (up to 30 min) operation with power levels of up to 0.8 MW and 0.5 MW, respectively. The output beam pattern has been measured and analyzed. The beam parameters are very close to those obtained in the first version of the gyrotron which shows a stable and reliable quasi-optical output system (see Table 1). Parasitic oscillations at a lower frequency (120 – 130 GHz) were observed which are supposed to be excited in the beam tunnel region and limit the performance of the gyrotron. After conditioning of the gyrotron, it was possible to operate the tube with a maximum power of about 0.72 MW for 3 min and

Table 1: Gaussian output beam parameters of the TED 140 GHz gyrotrons calculated from measured patterns.

Gyrotron	w_{0x}; w_{0y} beam waist	z_{0x}; z_{0y} location of beam waist	TEM_{00} [%]
Maquette	19.3; 17.4	-82.8; 61.2	95
Prototype	18.6; 21.3	202; 71	97
TED SN1	17.7; 21.6	126.9; 126.0	97.5
TED SN2	20.2; 22.5	103.5; 39.8	97
TED SN 2a	18.7; 22.2	127.0; 30.0	95
TED SN3	17.5; 20.6	130; 90	97
TED SN3a	17.6; 20.5	24; 77	96
TED SN 4	18.1; 18.5	105; 51	97

0.5 MW for 30 min, the specified 0.9 MW output power could not be achieved.

Acceptance tests of the serial gyrotron SN5 have been started at FZK. This tube has been equipped with a beam tunnel with a small modification of the inner contour which should suppress the excitation of parasitic oscillations. In short pulse operation the gyrotron delivered up to 0.95 MW. However, parasitic oscillations (120-130 GHz) were still limiting the performance of the tube. Furthermore and independent from the beam tunnel issue, the parameter optimization of this gyrotron had to be stopped as a shift of the mm-wave output beam at the window caused frequent arcing, raising the risk of a failure of the diamond disk.

The W7-X gyrotrons are optimized for single-frequency operation at 140 GHz, for details see ref. [8]. Their synthetic diamond windows have a resonant thickness of $4\lambda/2$ (1.8 mm) at 140 GHz and are also transparent at 105 GHz corresponding to $3\lambda/2$. Two modes, the $TE_{21,6}$ (103.8 GHz) and the $TE_{22,6}$ (106.3 GHz) exist in the vicinity of the desired frequency. Both modes could be exited by tuning the gyrotron magnetic field and adjusting the operation parameters (I_{beam} = 40 A and U_{acc} = 62 kV). We have focused on the $TE_{21,6}$ mode operation, because the output beam was almost perfectly centered at the output window, whereas the beam from the $TE_{22,6}$ mode was located somewhat off center. Using the TED prototype gyrotron a maximum output power of about 0.52 MW was achieved without collector voltage depression corresponding to an efficiency η = 21 %, which is compatible with theoretical predictions. The output power drops with increasing depression voltage while the efficiency increases from 21 % to 27 %. The corresponding collector loading at 0 and 8 kV depression voltage is 1.9 and 1.7 MW, respectively, which is incompatible with the collector-loading limit of 1.3 MW. Thus only operation at 0.4 MW with reduced beam current around 34 A can be handled safely. The mm-wave beam was transmitted through 7 mirrors of the quasi-optical transmission line into a calorimetric CW-load. Transmission losses of about 20 kW were measured, which compares well with the transmission loss fraction at 0.9 MW, 140 GHz operation. It is worth noting, that both the beam matching mirrors as well as the set of polarizers can be used without modification. Assuming, that all series gyrotrons behave similar to the prototype, the ECH&CD system of W7-X will be operated as a two-frequency system with a total power of 4 MW at the lower frequency. The operation range of experiments can then be extended towards different resonant magnetic fields of 1.86 T (X2 and O2 mode) and 1.25 T (X3 mode). An example for the O2-mode absorption at 103.8 GHz after 3 transits through the plasma is shown in Fig. 1 (bottom) as a function of plasma density and ECH power. The same transport code as for Fig. 1 (top) was used. An interesting parameter regime (absorption > 90 %) is accessible with moderate power at the reduced magnetic field. The calculated electron temperatures range from 3.5 to 5 keV, depending on plasma density and ECH power. Once plasma start-up could be achieved with the X3-mode, which is not clear yet, operation at 1.25 T is of particular interest, because ECH then could provide a target plasma for neutral beam injection heating for high-ß physics studies, which is most promising at low confining magnetic field.

4. High power tests of transmission system

The transmission system consists of single-beam waveguide (SBWG) and multi-beam waveguide (MBWG) components. For each gyrotron, a beam conditioning optics of five single-beam mirrors is used. Two of these mirrors match the gyrotron output to a Gaussian beam with the correct beam parameters. Two corrugated mirrors are used to set the appropriate polarization for optimum absorption of the radiation in the plasma. A fifth reflector directs the beam to a plane mirror array, the beam combining optics, which is situated at the input plane of a multi-beam waveguide (MBWG) [1]. The MBWG is designed to transmit up to seven beams from the gyrotron hall (entrance plane) to the stellarator hall (output plane). A mirror array separates the beams again at the output plane and distributes them via CVD-diamond vacuum barrier windows to the individually movable launchers in the W7-X torus. Two symmetrically arranged MBWGs are used to transmit the power of all gyrotrons. A major work package was the design completion and manufacturing of the transmission system near the torus. This comprises the reflectors type M13 and M14, which will be installed

in two "towers" in front of the W7-X ports as sketched in Fig. 5 (left). Both towers are completed, and the installation of control systems for reflectors and launchers, support structures, and granite absorbing plates has started, see Fig.5 (right).

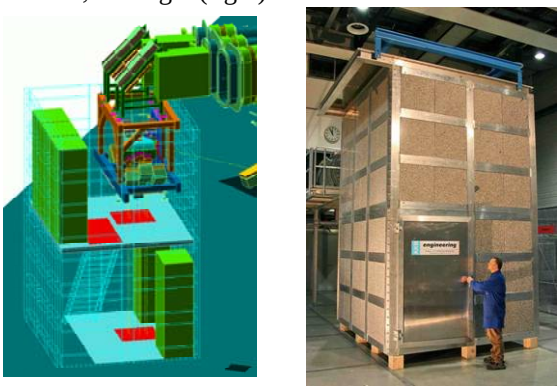

Fig. 5 Left: CAD sketch of the beam-distribution optics and control racks inside the two-storey tower. Right: ECH tower with mm-wave absorbing granite-wall structure.

Tests of the entire transmission line can only be performed, once the W7-X construction is completed and access to the main torus hall is provided. Therefore, we had installed retro-reflectors in the underground beam-duct in the image plane at half distance of the MBWG transmission line. Long-distance transmission can be simulated and tested by transmitting the high power mm-wave beams half way in forward direction and then back via the reflectors into the dummy load. First calorimetric high-power measurements are shown in Fig. 6, where the calorimetrically measured transmitted power is plotted versus the incident power. As a guide for the eye, the 'no-loss' line is also plotted. Total losses of 2.6±0.4% were measured for 10 reflections on the 2 x 3 MBWG mirrors and the 4 additional guiding mirrors over a total length of about 40 m.

The measured total losses are compared to the calculated losses for the individual components in Table 2. Good agreement is found with calculations and previous low power measurements. This result confirms the high quality of the quasi-optical concept for high power, long-distance transmission.

5. Summary

The ECH&CD system for W7-X is the most ambitious and largest CW plant presently under construction. It is designed to satisfy the physics demands for stationary heating and current drive at 2nd harmonic with X- and O-mode, 3rd harmonic with X-mode, as well as mode conversion heating in the high density regime with Bernstein modes. The 10 MW, CW mm-wave power from 10 gyrotrons is transmitted via an optical multi-beam waveguide system operating at atmospheric pressure, which is a unique feature of this system. The optical transmission offers favorable characteristics such as broadband transmission and a large margin for power handling. This allows operation of the system at two frequencies and with the option of a later power upgrade without modification of the transmission line.

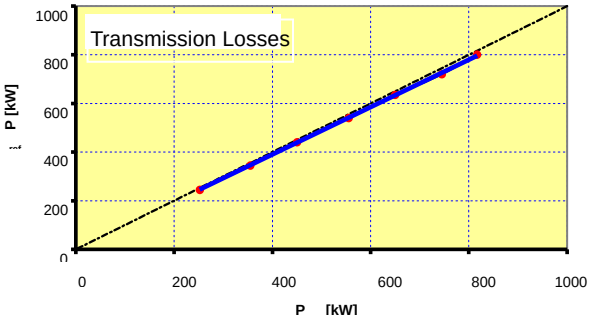

Fig. 6 Calorimetric measurement of the mm-wave power P_{refl} (after transmission through 10 mirrors) as a function of the incident power P_{inc}. The dashed-dotted line indicates no-loss transmission.

Tab. 2 Calculated transmission losses for different optical transmission components under normal atmospheric pressure (140 GHz). The sum of the different contributions is compared to the measured losses.

ITEM	OHMIC (%)	DIFFRACTION (%)	TOTAL (%)
M5, M6, M7	0.39	0.2	0.59
2 SR	0.26	0.1	0.36
M5, M6, M7	0.39	0.2	0.59
M4	0.13	0.1	0.23
SD	0.13	0.1	0.23
Atmospheric	0.68		0.68
SUM			**2.68**
MEASURED			**2.6 ± 0.4**

References

[1] V. Erckmann, *et al.*, Fus. Sci. and Techn., **52**, 291 (2007)

[2] N.B. Marushchenko, *et al.*, to be published in *Proc EPS 2007, Warsaw, Poland*

[3] M. Rome,*et al.*, Plas. Phys. Contr. Fus. **40,** 511 (1998)

[4] Yu. Turkin, *et al.*, to be published in *Proc EPS 2007, Warsaw, Poland*

[5] Yu. Turkin, *et al.*, Transport Simulations for W7-X. 33rd EPS Conference on Plasma Phys. Rome, 19 - 23 June 2006 ECA Vol.30I, P-2.113 (2006)

[6] H. P. Laqua, *et al.*, Phys. Rev. Lett. ***78***, 3467 (1997)

[7] B. Plaum, *et al.*, Fus. Sci. and Techn., ***50***, 1 *(2006)*

[8] M. Thumm *et al.*, IEEE Trans. Plas. Sci., **35**, 143 (2007)